An ANN-based smart capacitive pressure sensor in dynamic environment

Kot, Alex Chichung; Patra, Jagdish Chandra; Bos, Adriaan Van Den

2000

Patra, J. C., Bos, A. V. D., & Kot, A. C. (2000). An ANN-based smart capacitive pressure sensor in dynamic environment. Sensors and Actuators A: Physical, 86(1-2), 26-38.

https://hdl.handle.net/10356/94275

https://doi.org/10.1016/S0924-4247(00)00360-5

An ANN-based smart capacitive pressure sensor in dynamic environment

Jagdish C. Patra [a]*[1], Adriaan van den Bos [a], Alex C. Kot [b]

[a] Department of Applied Physics, Delft University of Technology, PO Box 5046, 2600 GA Delft, Netherlands
[b] Division of Information Engineering, School of Electrical and Electronic Engineering, Nanyang Technological University, Singapore 639798, Singapore
** Corresponding author.*
E-mail addresses: ejcpatra@ ntu.edu.sg (J.C. Patra), a.vandenbos@tn.tudelft.nl (A. van den Bos) , eackot@ntu.edu.sg (A.C. Kot) .

Abstract

A multilayer artificial neural network (ANN) is proposed for modeling of a capacitive pressure sensor (CPS). When the ambient temperature changes over a wide range, the nonlinear response characteristics of a CPS change significantly. In many practical conditions, the effect of temperature on the change in the CPS characteristics may be nonlinear. The proposed ANN model can provide correct readout of the applied pressure under such conditions. A novel scheme for estimation of the ambient temperature from the sensor characteristics itself is proposed. A second ANN is utilized to estimate the ambient temperature from the knowledge of the offset capacitance, i.e., the zero-pressure capacitance. A microcontroller unit (MCU)-based implementation scheme for this model is also considered. Simulation results show that this model can estimate the pressure with a maximum error of $\pm 2\%$ over a wide variation of temperature from -50 ℃ to 150 ℃.

Keywords: Smart pressure sensor; Artificial neural networks

1. Introduction

Capacitive pressure sensors (CPSs) are widely used because they have higher sensitivity and lower power dissipation than other pressure sensors. However, some of the difficulties associated with the CPS are: (i) its response characteristics are highly nonlinear, (ii) its change in capacitance is small compared to the offset capacitance, and (iii) its response characteristics change substantially when variation of operating temperature is large. Therefore, in a dynamic environment in which the ambient temperature undergoes large variation, the CPS needs appropriate compensation to

[1] On leave from the Department of Applied Electronics and Instrumentation Engineering, Regional Engineering College, Rourkela, Orissa 769 008, India. Dr. Patra joined the School of Electrical and Electronic Engineering, Nanyang Technological University, Singapore, as a Research Fellow in October 1999.

mitigate the adverse effects of the temperature besides corrections to its nonlinear characteristics.

Under such conditions, several signal processing techniques have been proposed for a CPS to obtain correct readout of the applied pressure [1–4]. These techniques include both iterative and non-iterative algorithms, and involve complex signal processing for the modeling of the CPS. They offer satisfactory performance unless the temperature variation is large and the influence of the temperature on the sensor characteristics is nonlinear.

Recently, artificial neural networks (ANNs) have emerged as a powerful learning technique to perform complex tasks in a dynamic environment. These networks are endowed with certain unique characteristics: the capability of universal approximation, the ability to learn from and to adapt to their environment, and the ability to cope with weak assumptions about the underlying physical phenomenon responsible for generation of input data. Another important property of the ANNs is its fault tolerance capability, because of which, graceful degradation of performance takes place if the network is partially damaged. Because of these characteristics, there have been numerous successful applications of ANNs in various fields of science, engineering and industry [5] including instrumentation and measurement [6,7] in general, and CPSs in particular [8–11].

Some of the applications of the ANNs in the field of instrumentation and measurement have been proposed [6,7]. To estimate the nonlinearity and for direct digital readout of a CPS, a simple functional link ANN (FLANN) has been employed [8]. A multilayer perceptron (MLP) has been proposed to model a CPS for estimation of applied pressure with a maximum of 1% full scale (FS) error over a temperature range from −20 ℃ to 70 ℃ [9]. A computationally efficient ANN has been proposed for modeling of a CPS operated under a wide variation of temperature to obtain accurate pressure readout with satisfactory performance [10]. However, in these papers, the effect of temperature on the sensor characteristics was assumed to be linear. An MLP-based compensation scheme for systematic uncertainities of the sensors subject to combined influence parameters using a second sensor has been proposed [11].

In the present paper, we propose a novel ANN-based model for a CPS operated under dynamic environment to provide accurate readout of the applied pressure. An MLP is proposed to model the CPS operated under temperature variations from −50 ℃ to 150 ℃. In agreement with practice, we have assumed that the temperature influences the sensor response characteristics nonlinearly. Next, a new scheme of estimation of the ambient temperature from the sensor characteristics itself, using a second MLP, is proposed. Through extensive simulation studies, good performance of this model is demonstrated. A microcontroller unit (MCU)-based scheme for implementation of the CPS model is also proposed.

2. Capacitive pressure sensor and switched capacitor interface

A CPS senses the applied pressure in the form of elastic deflection of its diaphragm. The capacitance of a CPS resulting from the applied pressure, P at the ambient temperature, T is given by:

$$C(P,T) = C_0(T) + \Delta C(P,T), \qquad (1)$$

where $\Delta C(P,T)$ is the change in capacitance and $C_0(T)$ is the offset capacitance, i.e., the zero-pressure capacitance, both at the ambient temperature T. The above capacitance may be expressed in terms of capacitances at the ambient temperature, T_0 as:

$$C(P,T) = C_0 f_1(T) + \Delta C(P,T_0) f_2(T), \qquad (2)$$

where, C_0 is the offset capacitance and $\Delta C(P,T_0)$ is the change in capacitance, both at the reference temperature. The functions $f_1(T)$ and $f_2(T)$, which are nonlinear functions of temperature, determine the effect of temperature on the sensor characteristics [2]. This model provides sufficient accuracy in determining the influence of temperature on the sensor response characteristics.

When pressure is applied to the CPS, its change in capacitance at the reference temperature, T_0 is given by:

$$\Delta C(P,T_0) = C_0 P_N \frac{1-\tau}{1-P_N}, \qquad (3)$$

where τ is the desensitivity parameter, P_N is the normalized applied pressure given by $P_N = P/P_{max}$, and P_{max} is the maximum permissible applied pressure. The parameters τ and P_{max} depend on geometrical structure and dimensions of the CPS. Since $\Delta C(P,T_0)$ becomes very large as P_N approaches 1, in practice, the value of P_N is normally kept within about 0.8.

In this study, in confirmation with practical conditions, we have considered that the ambient temperature influences the CPS characteristics nonlinearly. The nonlinear functions involved are $f_i(T)$, $i = 1$ and 2 and may be expressed as:

$$f_i(T) = 1 + g_i(T), \qquad (4)$$

where

$$g_i(T) = \eta_{i1} T_n + \eta_{i2} T_n^2 + \eta_{i3} T_n^3, \qquad (5)$$

$T_n = (T - T_0)/T_{max}$ and $\eta_{i,j}$, $i = 1$ and 2, and $j = 1$, 2, and 3, are the coefficients which determine the extent of nonlinear influence of the temperature on the sensor characteristics. Note that when $\eta_{i,j} = 0$ for $j = 2$ and 3, the influence of the temperature on the CPS response characteristics is linear. T_{max} is the maximum permissible temperature at which the sensor may be operated.

Let the normalized temperature, T_N be given by $T_N = T/T_{max}$. The normalized capacitance, C_N may be expressed as:

$$C_N = C(P,T)/C_0. \quad (6)$$

Using Eqs. (2) and (3), this may be rewritten as:

$$C_N = f_1(T) + \gamma f_2(T), \quad (7)$$

where $\gamma = P_N(1-\tau)/(1-P_N)$. Because of requirement of the ANN modeling, the C_N in Eq. (7) is divided by a factor of 2, so as to keep its maximum value within 1.

If the applied pressure is zero, then γ becomes zero. Therefore, the normalized zero-pressure capacitance, i.e., the normalized offset capacitance is given by:

$$C_{N0} = f_1(T) = 1 + g_1(T). \quad (8)$$

A switched capacitor interface (SCI) for the CPS is shown in Fig. 1. The CPS is represented by $C(P)$. The SCI output provides a voltage signal proportional to the capacitance change in the CPS due to applied pressure. The SCI operation can be controlled by a reset signal θ. When $\bar{\theta} = 1$ (logic 1), $C(P)$ charges to the reference voltage V_R while the capacitor C_S is discharged to ground. Whereas, when $\theta = 1$, the total charge $C(P)V_R$ stored in the $C(P)$ is transferred to C_S producing an output voltage given by:

$$V_O = KC(P), \quad (9)$$

where $K = V_R/C_S$. It may be noted that if ambient temperature changes, then the SCI output also changes, although the applied pressure remains the same. By choosing proper values of C_S and V_R, the normalized SCI output V_N may be obtained in such a way that

$$V_N = C_N. \quad (10)$$

The unnormalized and normalized SCI output for zero applied pressure are denoted by V_{00} and V_{N0}, respectively. Therefore, if $P_N = 0$, then $V_{N0} = C_{N0}$.

3. The multilayer perceptron and backpropagation algorithm

The multilayer perceptron is a feedforward network in which there may be one or more hidden layers besides one input and one output layer. Each layer may contain one or more nonlinear processing units called as a ‘neuron’, or a ‘node’. All layers, except the output layer, contain a bias or threshold node whose output is set to a fixed value of 1. All the nodes of a lower layer are connected to all the nodes of an upper layer through links called weights. The backpropagation (BP) algorithm, a generalized steepest descent algorithm, is the most popular learning technique used to train the MLP. The weights of the MLP are updated by using the BP algorithm during the training phase. The knowledge acquired by the network after learning is stored in its weights in a distributed manner. The MLP and the BP algorithm are briefly discussed below. For the details one may refer to [5].

Consider an L-layer MLP as shown in Fig. 2. In this network, the number of nodes in the input and output layers are N_0 and N_L, respectively. The number of nodes in the hidden layers is denoted by N_l where $l = 1, 2, \ldots, L-1$. The architecture of an L-layer MLP is denoted by $N_0 - N_l$- ... -N_{L-1} $-N_L$. During training phase, an input pattern and its corresponding desired or target pattern is applied to the network. At the kth instance, let the input pattern applied to the MLP be denoted by $\{u_i(k)\}$, where $i = 1, 2, \ldots, N_0$. No computation takes place in the input layer of the MLP and hence, the node output for this layer is given by $x_i^{(0)} = u_i(k)$. The node outputs for other layers at the kth instance are given by:

$$x_i^{(l)} = \rho\left(S_i^{(l)}\right) \tag{11}$$

for $l = 1, 2, \ldots, L$, and $i = 1, 2, \ldots, N_l$, where,

$$S_i^{(l)} = \sum_{j=0}^{N_{l-1}} x_j^{(l-1)} w_{ij}^{(l)}, \tag{12}$$

$x_i^{(l-1)}$ is the ith node output of the $(l-1)$th layer, $w_{ij}^{(l)}$ is the connection weight from the jth node of $(l-1)$th layer to ith layer of lth layer, and $x_0^{(l)}$ is the bias unit whose output is set to 1. The most popular nonlinear function $\rho(\cdot)$ is given by

$$\rho(z) = \tanh(z) = \frac{1 - \exp(-2z)}{1 + \exp(-2z)}. \tag{13}$$

Let the output of the MLP, and the target output at the kth instant be represented by $\{y_i(k)\}$ and $\{d_i(k)\}$, where $i = 1, 2, \ldots, N_L$, respectively. Then, $y_i(k) = x_i^{(L)}$. The error at the kth instant is given by

$$e_i(k) = d_i(k) - y_i(k). \tag{14}$$

Thus, the sum of square errors produced by the MLP is given by

$$E(k) = \sum_{i=1}^{N_L} \left[e_i(k)\right]^2. \tag{15}$$

The BP algorithm attempts to minimize the cost function $E(k)$. recursively by updating the weights of the network. The algorithm for weight update at the kth instant is given by:

$$w_{ij}^{(l)}(k+1) = w_{ij}^{(l)}(k) + \alpha \Delta_{ij}(k) + \beta \Delta_{ij}(k-1), \tag{16}$$

where,

$$\Delta_{ij}(k) = \delta_i^{(l)} x_j^{(l-1)} \quad \text{for } l = L, L-1, \ldots, 1, \tag{17}$$

$$\delta_i^{(l)} = e_i(k)\rho'\left(S_i^{(l)}\right) \quad \text{for } l = L, \tag{18}$$

$$\delta_i^{(l)} = \left(\sum_{j=1}^{N_{l+1}} \delta_j^{(l+1)} w_{ji}^{(l+1)}(k) \right) \rho'\left(S_i^{(l)}\right)$$

for $l = L-1, L-2, \ldots, 1$. (19)

The BP algorithm is a generalized form of steepest descent algorithm that attempts to find optimum weights to minimize the chosen cost function [5]. The partial derivative of the hyperbolic tangent function with respect S is denoted by $\rho'(S)$. The so-called learning rate and the momentum rate are denoted by α and β, respectively, and their values should lie between 0 and 1.

4. The MLP-based CPS model

In certain systems, such as missiles, aircrafts, and chemical and process industries, the CPS may be operated in a dynamic environment in which the temperature variation may be quite large. Further, the influence of temperature on the CPS characteristics is often nonlinear. To cope with these conditions, we propose an ANN-based model to take care of a large variation of temperature ranging from −50 ℃ to 150 ℃.

The proposed scheme of the ANN-based CPS model for estimation of applied pressure is shown in Fig. 3. This is analogous to the channel equalization scheme used in a digital communication receiver to cancel the adverse effects of the channel on the data being transmitted [5]. To obtain direct digital readout of the applied pressure, an inverse model of the CPS may be used to compensate adverse effects of the nonlinear characteristics, and its variations due to change in temperature. For this purpose, an ANN is utilized to obtain the inverse model of the CPS.

In this ANN-based CPS model, all the signals used for training and testing are suitably scaled by appropriate scale factors (SFs) to keep their range within ±1.0. The model operates in two phases: the training phase and the test phase. In the training phase, the ANNs used in the model are trained to learn the sensor characteristics and the environment. The pressure-ANN (P-ANN) is used for learning the sensor response characteristics and their nonlinear temperature interaction, whereas the temperature-ANN (T-ANN) is used for learning the variations of the temperature in the environment.

Several data-sets are needed to train the ANNs. An input pattern and its corresponding desired, or target pattern constitute one pair of data in the data-set. The available data-sets are segregated into two parts. The first part, called as training-set, is used for training of the ANNs, and the other part called the test-set, is used for testing of the model to verify its effectiveness.

During the training phase, an input pattern from the training-set is applied to the ANN. Then, the output of the ANN is computed. This output is compared with the corresponding target pattern. The error obtained from this comparison is then used to update the weights of the ANN using the BP algorithm described in Section 3. This training procedure continues till the error reaches a preset minimum value. Next, the final

weights are stored in an EPROM which are used during testing and actual use of the sensor model.

During the second phase, i.e., the test phase, the stored final weights are loaded into the ANNs. An input pattern from the test-set is applied to the ANN model and its output is computed. If the ANN output and the target pattern match closely, then it may be said that the ANN model has learned the sensor characteristics satisfactorily.

4.1. Training phase — pressure

In the first stage, the MLP is used to learn the CPS response characteristics. The scheme for this is shown in Fig. 3 (a). In this case, the inputs to the P-ANN consist of the normalized temperature (T_N) and the normalized SCI output (V_N). The desired (or the target) output for the network is the normalized applied pressure (P_N). One data-set for a specific temperature is obtained by recording the SCI output (V_N) for different values of applied pressure, covering the operating range of the sensor at that temperature. Next, at different temperature values, covering the full operating range, data-sets are generated. The P-ANN is trained by taking the patterns from the training-set, and its weights are updated by using the BP algorithm. After training, the weights of the ANN are frozen and stored in an EPROM. In what follows, the final weights are denoted by W_P.

4.2. Training phase — temperature

The scheme of estimation of the ambient temperature by using another MLP from the knowledge of sensor characteristics itself is shown in Fig. 3 (b). From Eq. (8), it may be seen that C_{N0} contains temperature information. However, since the influence of the temperature on the CPS characteristics is considered to be nonlinear, the temperature information cannot be obtained from the knowledge of C_{N0} using this equation directly. The MLP may be trained by inputting the values of $C_{N0,}$ i.e., the values of $V_{N0.}$ The desired or target output is the normalized temperature values, T_N. Using the BP algorithm, the weights of the T-ANN are updated. After the training is complete, the final weights are stored in an EPROM. In what follows, the final weights are denoted by W_T.

4.3. Test phase — the complete model

The complete scheme of the MLP-based model is shown in Fig. 3 (c). This model can estimate the applied pressure accurately independent of temperature variation and its nonlinear interaction with the CPS characteristics. During test-phase, and actual use, the weights W_P and W_T, stored in the EPROM are loaded into the P-ANN and T-ANN, respectively. The P-ANN has learned the inverse characteristics of the CPS at different values of temperature, and this knowledge has been stored in its weights in a distributive manner. The T-ANN has learned about the changes in the environment. The temperature information needed for the P-ANN is obtained from the T-ANN. The T-ANN gets its input from the value of $V_{N0,}$ i.e., from the normalized SCI output at zero applied pressure. Next, the input patterns from the test-set are applied, and the model output ($\widehat{P}_N$) is computed. If the model output matches closely with the actual applied pressure (P_N), then it may be said that the ANN has learned the CPS characteristics correctly. Then, the model can be used in practice to estimate the pressure and to obtain its readout.

5. Simulation studies

We have carried out extensive simulation studies to evaluate the performance of the proposed ANN-based CPS model. In the following we describe the details of the simulation study.

5.1. Preparation of data-sets

All the parameters of the CPS, such as, ambient temperature, applied pressure, and the SCI output voltage, used in the simulation study were suitably normalized so as to keep their values within ±1.0. Appropriate scale factors (SFs) were chosen for this purpose. Several data-sets are needed for training as well as for testing of the ANN model. These data-sets were generated as follows. The SCI output voltage (V_N) was recorded (refer Eq. (10)) at the reference temperature (25 ℃) at different known values of normalized pressure (P_N) chosen between 0.0 and 0.6 at an interval of 0.05. Thus, these 13 pairs of data (P_N and V_N) constitute one data-set at the reference temperature. To study the influence of temperature on the CPS characteristics, we have considered three forms of nonlinearities denoted by NL1, NL2, and NL3, and the linear form denoted by NL0 (refer Eq. (4)). These are simulated by choosing proper values of η_{ij} in Eq. (5). The corresponding values of η_{ij} are tabulated in Table 1.

Next, with the knowledge of the data-set at reference temperature, and the chosen values of η_{ij}, and using Eq. (7), the response characteristics of the CPS for a specific ambient temperature were generated. Each of these response characteristics consists of 13 pairs of data (P_N and V_N), and corresponds to a data-set at that temperature. For a temperature range from −50 ℃ to 150 ℃, at an increment of 10 ℃, 21 data-sets, each containing 13 data pairs were generated. Next, these data-sets were divided into two groups: the training-set and the test-set. The training-set, used for training of the ANNs, consists of five data-sets corresponding to −50 ℃, 0 ℃, 50 ℃, 100 ℃, and 150 ℃, and the remaining 16 data-sets constitute the test-set.

The response characteristics of the CPS for different values of temperature are shown in Fig. 4. It may be observed from this figure that wide variation in the sensor characteristics occurs when the ambient temperature changes from −50 ℃ to 150 ℃. Further, the response characteristics change differently for different forms of chosen nonlinearities.

5.2. Training and testing of the P-ANN

A 2-layer MLP with 2-5-1 architecture was chosen in this modeling problem (see Fig. 3(a)). The two inputs to the MLP were the normalized temperature (T_N) and the normalized SCI output voltage (V_N). The desired output of the MLP was the normalized pressure (P_N).

Initially, all the weights of the P-ANN were set to some random values within ±0.5. During training, the five data-sets were chosen randomly. Further, the individual patterns of each set were also selected in a random manner. After application of one input pattern, the P-ANN produces an output $\widehat{P}_N$, which was compared with the which was compared

with the target pattern to obtain an error value. This error was used to update the weights of the MLP by using the BP algorithm discussed in Section 3. The values of the learning parameter α, and the momentum factor β, of Eq. (16) were chosen as 0.5 and 0.7, respectively. Next, another pattern was applied, and this process continues till the mean square error between the desired and the P-ANN output reaches a minimum value. Completion of weight adaptation for the 13 data pairs of all the five training-sets constitute one iteration. For effective learning, 30,000 iterations were made to train the MLP model. In the end, the final weights of the *P*-ANN (W_{P}) were stored for later use for performance evaluation and actual use of the model. This procedure was repeated for the linear as well as three chosen nonlinear forms of temperature interaction with CPS characteristics (NL0, and NL1–NL3). The four sets of the final weights of the P-ANN model are provided in Table 2.

The performance evaluation of the model was carried out by loading the final stored weights into the MLP. It may be noted that, during testing, and actual use of the CPS model, there is no updating of the weights. The inputs are applied to the model, and the ANN estimates the applied pressure from the knowledge of the stored weights loaded into it. For testing purpose, the SCI output voltage was simulated with a range starting from 0.35 to 0.80 with an increment of 0.001, and then applied to the model along with the temperature information. To evaluate the effectiveness of the model, the ANN output ($\widehat{\mathrm{P}}_N$) was computed and then compared with the true values of applied pressure (P_{N}).

5.3. Training and testing of the T-ANN

The T-ANN is used for the estimation of the ambient temperature from the known values of C_{N0} corresponding to different temperatures. For the chosen values of η_{ij} (see Table 1), the variation of C_{N0} with the change in temperature for the linear (NL0) and the three forms of nonlinear interactions (NL1–NL3) is shown in Fig. 5. The *T*-ANN is employed to learn these nonlinear functions for estimation of ambient temperature.

An MLP with 1-5-1 architecture was chosen for this purpose. During training, the values of C_{N0} corresponding to -50 ℃, 0 ℃, 50 ℃, 100 ℃ and 150 ℃ were chosen as training-set (the same set was used for training the P-ANN). The input and target output of the T-ANN were the values of C_{N0} and T_{N}, respectively (see Fig. 3 (b)).

After application of the input and the corresponding target output to the *T*-ANN, its weights were updated using the BP algorithm. Since the MLP has to learn the nonlinear functions from only five observations, sufficiently large iterations were chosen for complete training. Both the values of α and β were chosen as 0.7. The updating of the weights were continued up to 100,000 iterations. The four sets of final weights, W_{T} corresponding to the linear and the three nonlinear forms of interactions are tabulated in Table 3.

The testing of the T-ANN was carried out after loading the stored weights into the network. The value of C_{N0} was varied from 0.35 to 0.60 with an increment of 0.001 and fed to the MLP. The output of the T-ANN and the true value of the normalized temperature were compared to verify the performance of the model.

6. Results and discussion

Here, we provide the performance results of the simulation study for estimating the applied pressure and the ambient temperature.

6.1. Estimation of pressure

True and estimated pressures at different values of temperature taken from test-set for the linear and the three nonlinear forms, i.e., NL0, and NL1–NL3, respectively, are plotted in Fig. 6. Here, different symbols represent true normalized pressure whereas, the dotted lines denote the estimated pressure. Similar plots for temperature values taken from training-set are shown in Fig. 7. It may be noted that the P-ANN has not seen the sensor characteristics for the values of temperature taken from the training-set. From these two figures, it may be observed that, the MLP is capable of estimating the applied pressure quite accurately for the full range of applied pressure from 0.0 to 0.6. Even, it is capable of predicting the applied pressure for the range beyond 0.6, although the network was not trained for this range of P_N.

The plots of the true versus and the estimated pressure at different values of temperature taken from test-set for NL0 and NL1–NL3 are shown in Fig. 8. The linearity of estimation in the case of NL0 is quite good. In the cases of nonlinear interactions, NL1–NL3, the linearity will be satisfactory for most applications.

The full scale percent error was computed as hundred times the difference between the true and estimated pressure. For the whole range of applied pressure from 0.0 to 0.6, the maximum FS error for the linear form, NL0 remains within ±1.0%; whereas, in the nonlinear forms, the maximum FS error remains within ±2.0%. For the whole temperature range from −50 ℃ to 150 ℃, at specific values of applied pressure (i.e., P_N = 0.1,0.3, and 0.5), the values FS error were plotted for NL0 and NL1–NL3 in Fig. 9. It may be seen that for the whole range of temperature variation, the maximum FS error in the case of the linear and the three nonlinear forms of interaction, remains within ±1% and ±2%, respectively.

From the above findings, it may be concluded that the performance of the MLP model for estimation of pressure is excellent in the linear form of interaction and it is quite satisfactory for the three forms of nonlinear interaction of temperature on the CPS characteristics.

6.2. Estimation of temperature

Plots of the estimated and the true temperature as a function of the normalized capacitance for the linear (NL0) and three nonlinear forms (NL1–NL3) are shown in Fig. 10. Here, the ‘dots’ represent the true temperature and the ‘dotted line’ represents the estimated temperature. Close agreement between the two values is quite evident from these plots. The absolute errors in estimation of temperature for the four cases are plotted in Fig. 11. For the whole range of temperature variation from −50 ℃ to 150 ℃, the maximum error of estimation remains within ±2 ℃ for both NL0 and NL3. Whereas, for NL1 and NL2, it remains within ±5 ℃ and ±3 ℃, respectively. From these observations, effective performance of the T-ANN is quite evident.

7. An implementation scheme

Due to rapid decrease in unit cost and fast increase in on-chip capabilities, the MCUs have been found quite suitable for use in a various intelligent systems. Currently available MCUs can be configured with all the required RAM/ROM/EEROM as well as serial interface and multiple channel A/D conversion support chips.

To estimate the ambient temperature from the sensor characteristics itself, we propose the following scheme. The training of the ANNs are carried out off-line and their corresponding weights are stored in the EEROM of the MCU.

In practical use of a CPS there is only one measured signal, i.e., V_N. Therefore appropriate arrangements are to be made to obtain the signals separately for estimation of temperature and pressure. The on-line estimation of pressure using this ANN-based scheme consists of a measurement cycle. Each of the measurement cycle consists of a *t_est* and a *p_est* cycle. In the *t_est* cycle the ambient temperature is estimated whereas, in the *p_est* cycle the applied pressure is estimated. During *t_est* cycle, provision is made to separate out the CPS from the applied pressure, and then the zero-pressure capacitance (V_{N0}) is measured. From the knowledge of (V_{N0}), the ambient temperature can be estimated using *T*-ANN (see Fig. 3 (c)). Next, during the *p_est* cycle, the pressure is applied to the CPS, and V_N is measured. Now, using this measured value and the estimated temperature, the pressure is estimated using Fig. 3 (c). Appropriate control and logic circuits are to be implemented in the MCU for this measurement scheme.

A scheme of implementation of the MLP-based CPS model using an MCU is depicted in Fig. 12. The SCI converts the change in capacitance of the CPS due to applied pressure into an equivalent voltage level. This analog SCI voltage is passed through an ADC. The digital temperature information is similarly obtained from the knowledge of C_{N0}.

During the training-phase, the CPS is operated under controlled temperature and the data pairs so collected can be stored in the memories of the MCU. These training data can be fed to a PC connected to the MCU during training of the MLP-based model. After completion of training, the weights of the MLP are stored in the EEROM of the MCU. With the available hardware, such as adders and multipliers of the MCU, the MLP-based model can be implemented in the MCU. The digital readout of the applied pressure can be displayed through the data bus.

8. Conclusions

We have proposed a novel and effective ANN-based scheme for modeling a capacitive pressure sensor operated in a dynamic environment. When the ambient temperature changes over a wide range, the nonlinear response characteristics of the CPS undergo change in a complex manner. A switched capacitor interface circuit is proposed to convert the CPS output in terms of a voltage signal. At different ambient temperatures, few data points from the sensor characteristics were obtained. These data were then used to train the MLP model using the back propagation algorithm. The training of ANNs may

be carried out off-line and the final ANN weights can be stored in an EPROM. After training, the MLP model is capable of estimating the applied pressure accurately irrespective of nonlinear characteristics of the CPS and its nonlinear dependence on temperature.

Using a second MLP, we have presented a novel scheme for estimating the ambient temperature from the knowledge of the sensor characteristics itself. The values of offset capacitance, at different ambient temperature were used to train this MLP. This MLP is capable of estimating the ambient temperature quite accurately. During practical use of the CPS, first, the ambient temperature is to be estimated. This is made by feeding the value of the offset capacitance to the second MLP. Next, the estimated temperature along with the output of the CPS is fed to the first MLP model to estimate the applied pressure.

The on-line estimation of the applied pressure is carried out in a measurement cycle which consists of a *t_est* cycle and a *p_est* cycle for estimation of the ambient temperature and the applied pressure, respectively. Appropriate logic and control circuits may be implemented in the MCU to carry out the measurement cycle.

We have considered different forms of nonlinear interaction of temperature on the sensor characteristics with a temperature range from −50 ℃ to 150 ℃. The accuracy of the ANN model for estimation of pressure remains within ±2% (FS). The maximum absolute error in estimation of temperature remains within ±5 ℃. The proposed MLP-based model can be easily implemented using a microcontroller unit. Such ANN-based models may be applied to incorporate intelligence in other fields of instrumentation and measurement.

9. Acronyms used

A/D	Analogue to digital
ADC	Analogue to digital converter
ANN	Artificial neural network
BP	Backpropagation
CPS	Capacitive pressure sensor
EEROM	Electrically erasable read only memory
EPROM	Electrically programmable read only memory
FS	Full scale
MCU	Micro-controller unit
MLP	Multilayer perceptron

P-ANN	Pressure-ANN
RAM	Random access memory
ROM	Read only memory
SCI	Switched capacitor interface
SF	Scale factor
T-ANN	Temperature-ANN

References

[1] M. Yamada, T. Takebayashi, S.-I. Notoyama, K. Watanabe, A switched-capacitor interface for capacitive pressure sensors, IEEE Trans. Instrum. Meas. 41 (1) (1992) 81–86.

[2] M. Yamada, K. Watanabe, A capacitive pressure sensor interface using oversampling $\Delta - \Sigma$ demodulation techniques, IEEE Trans. Instrum. Meas. 46 (1) (1997) 3–7.

[3] K.F. Lyahou, G. van der Horn, J.H. Huijsing, A noniterative polynomial 2-D calibration method implemented in a microcontroller, IEEE Trans. Instrum. Meas. 46 (4) (1997) 752–757.

[4] X. Li, G.C. Meijer, G.W. de Jong, A microcontroller-based self-calibration technique for a smart capacitance angular-position sensor, IEEE Trans. Instrum. Meas. 46 (4) (1997) 888–892.

[5] S. Haykin, Neural Networks, Maxwell Macmillan, Ontario, Canada, 1994.

[6] L.F. Pau, F.S. Johansen, Neural network signal understanding for instrumentation, IEEE Trans. Instrum. Meas. 39 (4) (1990) 588–594.

[7] P. Daponte, D. Grimaldi, Artificial neural networks in measurements, Measurement 23 (1998) 93–115.

[8] J.C. Patra, G. Panda, R. Baliarsingh, Artificial neural network-based nonlinearity estimation of pressure sensors, IEEE Trans. Instrum. Meas. 43 (6) (1994) 874–881.

[9] J.C. Patra, An artificial neural network-based smart capacitive pressure sensor, Measurement 22 (3-4) (1997) 113–121.

[10] J.C. Patra, A. van den Bos, Modeling of an intelligent pressure sensor using functional link artificial neural networks, ISA Transactions, in press.

[11] P. Arpaia, P. Daponte, D. Grimaldi, L. Michaeli, Systematic error correction for experimentally modeled sensors by using ANNs, Proc. IEEE IMTC'99, Venice, May 1999, pp. 1635–1640.

Biographies

Jagdish Chandra Patra was born on January 15, 1957 in Nowrangpur, Orissa, India. He received his BSc (Engg.) and MSc (Engg.) degrees in Electronics and Telecommunication Engineering from Sambalpur University, Orissa in 1978 and 1989, respectively. He earned his PhD degree from the Department of Electronics and Electrical Communication Engineering, Indian Institute of Technology, Kharagpur in 1996. After obtaining his Bachelor's degree, Dr. Patra served different teaching, research and development, and Industrial organizations. In 1987, he joined as a lecturer in the Department of Electrical Engineering, Regional Engineering College, Rourkela, Orissa. In 1990, he was promoted to Assistant Professor in the Department of Applied Electronics and Instrumentation Engineering of this College and till now he is continues as such. Dr. Patra was a Guest Teacher (Gastdocent) in the Department of Applied Physics, Delft University of Technology, The Netherlands from April–October 1999. Now, he has joined the Nanyang Technological University, Singapore, as a Research Fellow by taking leave from his parent College. Dr. Patra has published several research papers in reputable national and international journals. His research interest includes signal processing using intelligent techniques such as artificial neural networks, fuzzy logic and genetic algorithms. He is a member of the IEEE (USA), Institution of Engineers (India) and a life member of Indian Society for Technical Education.

Adriaan van den Bos is full professor of Physics at Delft University of Technology, Delft, The Netherlands. At the same institute he was awarded the Physics Engineering degree and the Doctor of Technical Sciences degree in 1962 and 1974, respectively. Professor Van den Bos is author of more than 40 journal papers, one of which has become a Citation Classic.

Alex C. Kot was educated at the University of Rochester, New York, and at the University of Rhode Island, Rhode Island, USA, where he received the PhD degree in Electrical Engineering in 1989. He was with the AT&T Bell, New York and URI, USA. Since 1991, he has been with the Nanyang Technological University (NTU), Singapore, where he is currently Head of the Information Engineering Division, School of Electrical and Electronic Engineering. His research and teaching interests are in the areas of digital signal processing, communications and statistical signal processing. Dr. Kot has published more than 60 technical papers in journals and conference proceedings. He has also received the NTU Best Teacher of the Year Award and has served as the Chairman of the IEEE Signal Processing Chapter in Singapore.

List of Tables

List of Figures

Fig. 10. True and estimated values of temperature: (a) NL0; (b) NL1; (c) NL2; (d) NL3.

Fig. 11. Absolute error in estimation of temperature: (a) NL0, NL1; (b) NL2, NL3.

Fig. 12. A scheme of MCU-based implementation of the model.

NL form	η_{11}	η_{12}	η_{13}	η_{21}	η_{22}	η_{13}
NL0	−0.20	0.00	0.00	0.70	0.00	0.00
NL1	−0.20	0.20	−0.10	0.70	−0.30	0.40
NL2	−0.20	0.05	−0.20	0.70	−0.10	−0.50
NL3	−0.20	−0.10	−0.07	0.70	0.10	−0.30

Table 1

Weights	NL0	NL1	NL2	NL3
w_{10}	1.214	2.069	1.535	1.532
w_{11}	−0.141	−0.382	1.348	−0.420
w_{12}	−2.991	−5.363	−3.113	−1.842
w_{20}	0.092	0.097	0.059	0.056
w_{21}	0.003	0.000	−0.052	−0.155
w_{22}	−0.159	−0.157	−0.079	−0.090
w_{30}	−2.785	−3.104	−3.808	−3.522
w_{31}	1.257	3.123	2.044	1.118
w_{32}	7.744	9.016	8.429	7.697
w_{40}	−0.783	−0.821	−1.854	−0.983
w_{41}	0.165	−0.091	1.195	1.205
w_{42}	1.125	1.382	0.268	−0.720
w_{50}	1.455	1.758	0.797	1.987
w_{51}	0.746	0.392	0.014	0.262
w_{52}	−1.368	−1.684	−2.964	−3.349
v_0	−1.272	−1.699	−0.228	0.177
v_1	−0.457	−0.882	−0.228	0.219
v_2	−0.058	−0.043	0.023	0.132
v_3	1.762	1.707	0.642	0.587
v_4	0.408	0.403	0.741	0.430
v_5	−0.424	−0.525	−0.888	−0.590

Table 2

Weights	NL0	NL1	NL2	NL3
w_{10}	−3.160	−3.004	−1.662	−1.366
w_{11}	4.582	4.261	3.197	5.315
w_{20}	1.697	1.094	1.088	1.476
w_{21}	−2.802	−2.316	−2.122	−3.068
w_{30}	2.189	2.477	1.023	1.414
w_{31}	−3.301	−3.622	−1.999	−2.943
w_{40}	0.675	0.984	0.120	0.338
w_{41}	−1.289	−2.056	−0.239	−0.676
w_{50}	−3.085	−9.922	−3.903	−5.245
w_{51}	9.625	24.212	8.350	8.276
v_0	1.152	3.621	0.401	−0.166
v_1	−1.303	−1.108	0.090	−1.431
v_2	0.259	−0.253	−0.057	−0.003
v_3	0.463	0.410	−0.053	0.018
v_4	0.104	−0.215	−0.006	0.059
v_5	−2.398	−4.665	−0.992	−1.894

Table 3

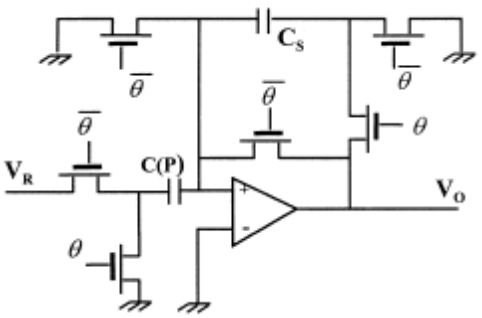
C_S
$\overline{\theta}$
$\overline{\theta}$
$\overline{\theta}$
θ
$\overline{\theta}$
V_R
C(P)
V_O
+
-
θ

Fig. 1

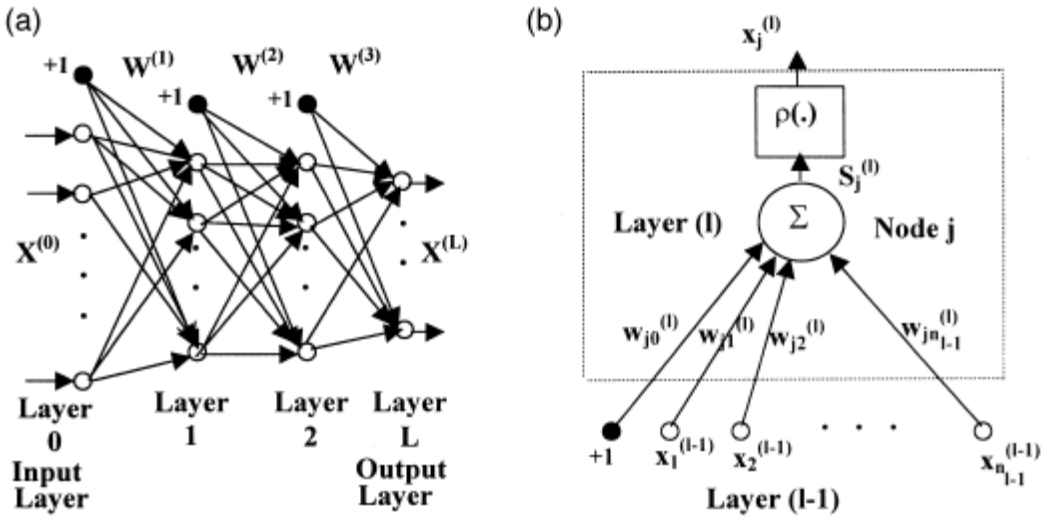
(a)
+1
W(1)
W(2)
W(3)
+1
+1
X(0)
X(L)
Layer 0
Input Layer
Layer 1
Layer 2
Layer L
Output Layer
(b)
xj(l)
ρ(.)
Sj(l)
Layer (l)
Σ
Node j
wj0(l)
wj1(l)
wj2(l)
wjnl-1(l)
+1
x1(l-1)
x2(l-1)
xnl-1(l-1)
Layer (l-1)

Fig. 2

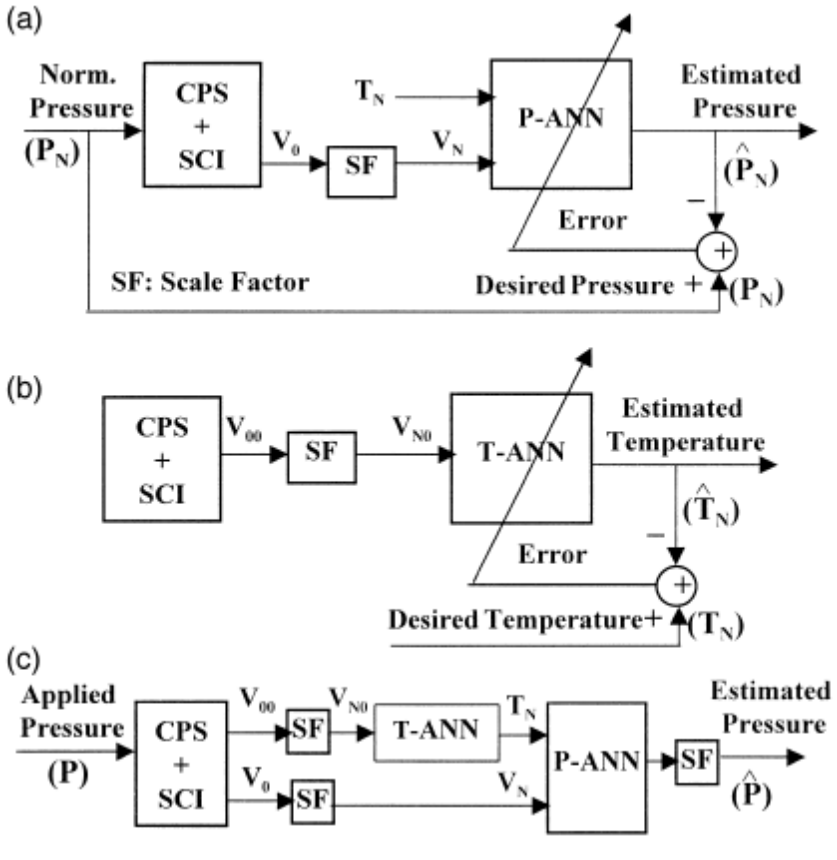
(a)
Norm. Pressure
(P_N)
CPS + SCI
V_0
SF
T_N
V_N
P-ANN
Estimated Pressure
(P̂_N)
Error
SF: Scale Factor
Desired Pressure
(P_N)
(b)
CPS + SCI
V_00
SF
V_N0
T-ANN
Estimated Temperature
(T̂_N)
Error
Desired Temperature
(T_N)
(c)
Applied Pressure
(P)
CPS + SCI
V_00
SF
V_N0
T-ANN
T_N
V_0
SF
V_N
P-ANN
SF
Estimated Pressure
(P̂)

Fig. 3

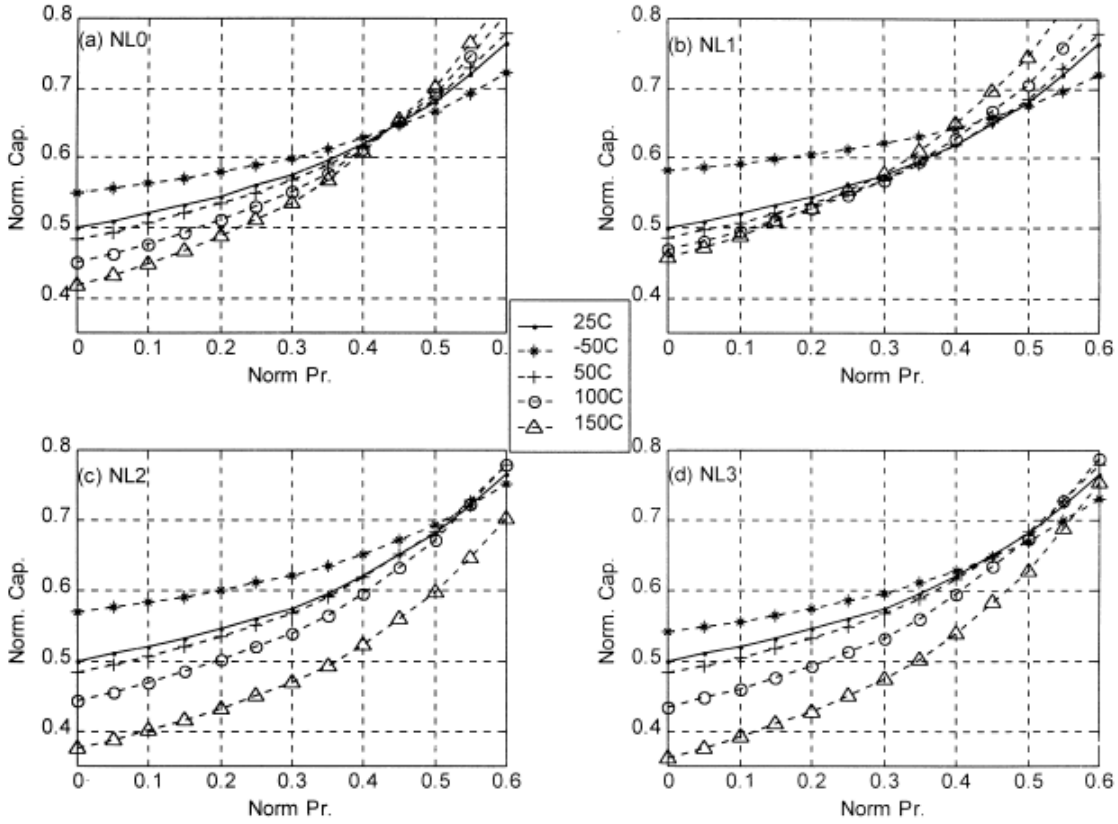

Fig. 4

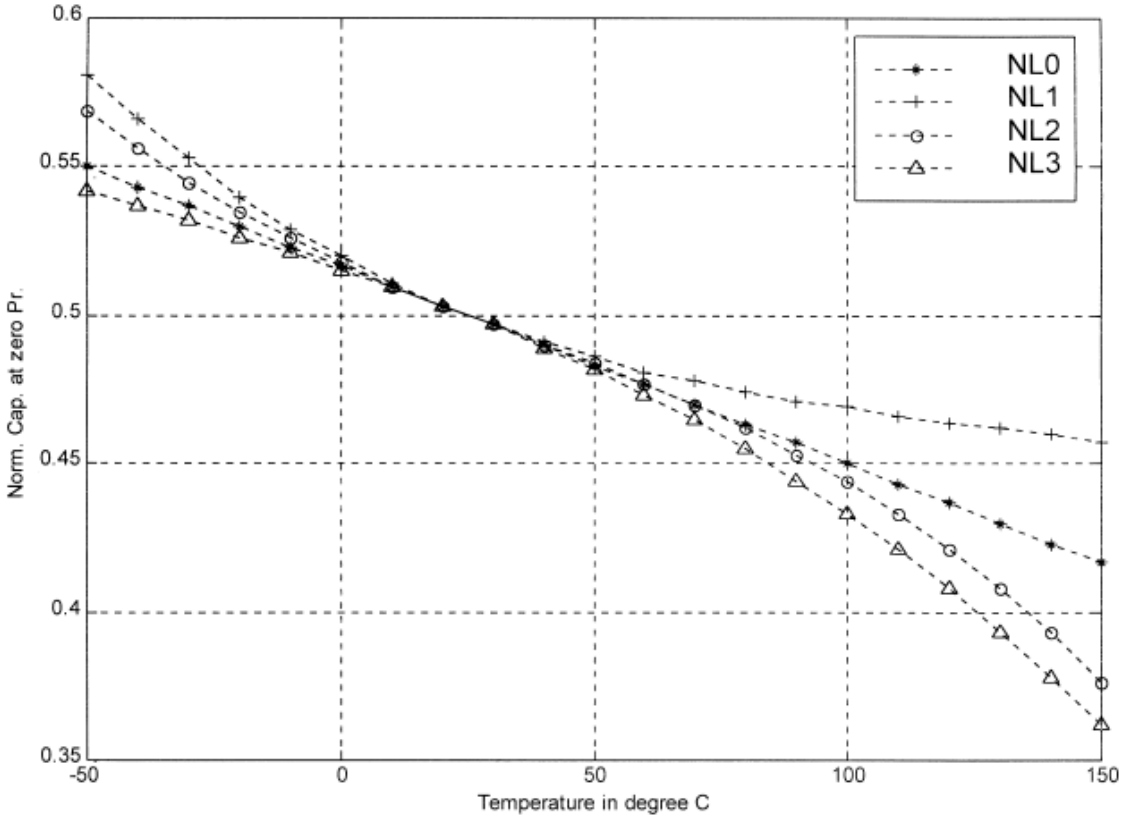
NL0
NL1
NL2
NL3
Norm. Cap. at zero Pr.
Temperature in degree C
0.6
0.55
0.5
0.45
0.4
0.35
-50
0
50
100
150

Fig. 5

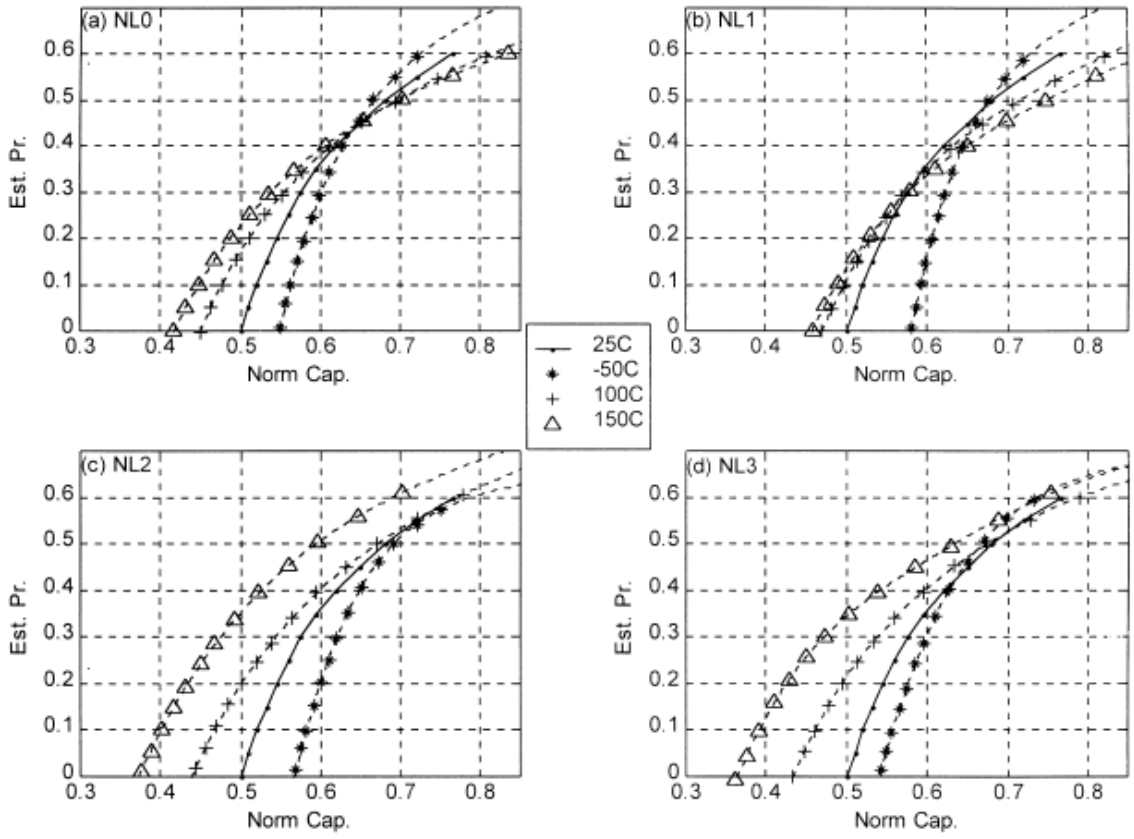

Fig. 6

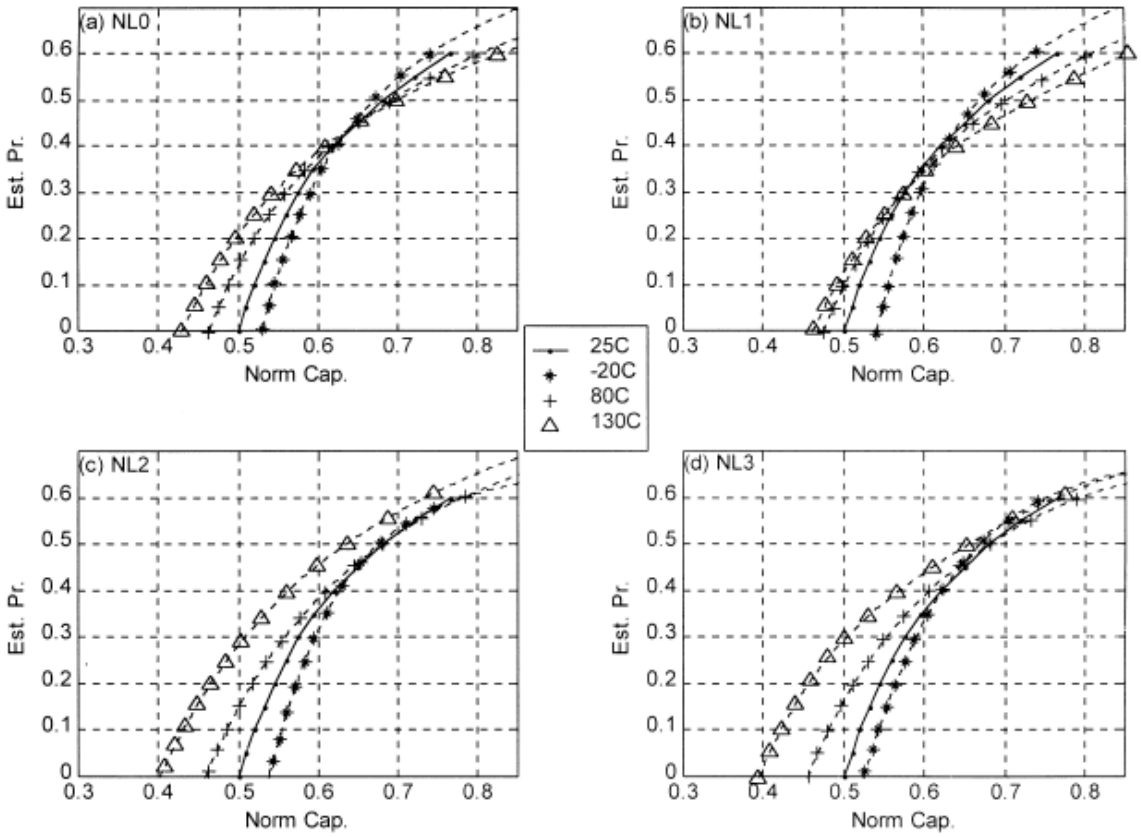
(a) NL0
(b) NL1
(c) NL2
(d) NL3
Est. Pr.
Norm Cap.
0
0.1
0.2
0.3
0.4
0.5
0.6
0.3
0.4
0.5
0.6
0.7
0.8
25C
-20C
80C
130C

Fig. 7

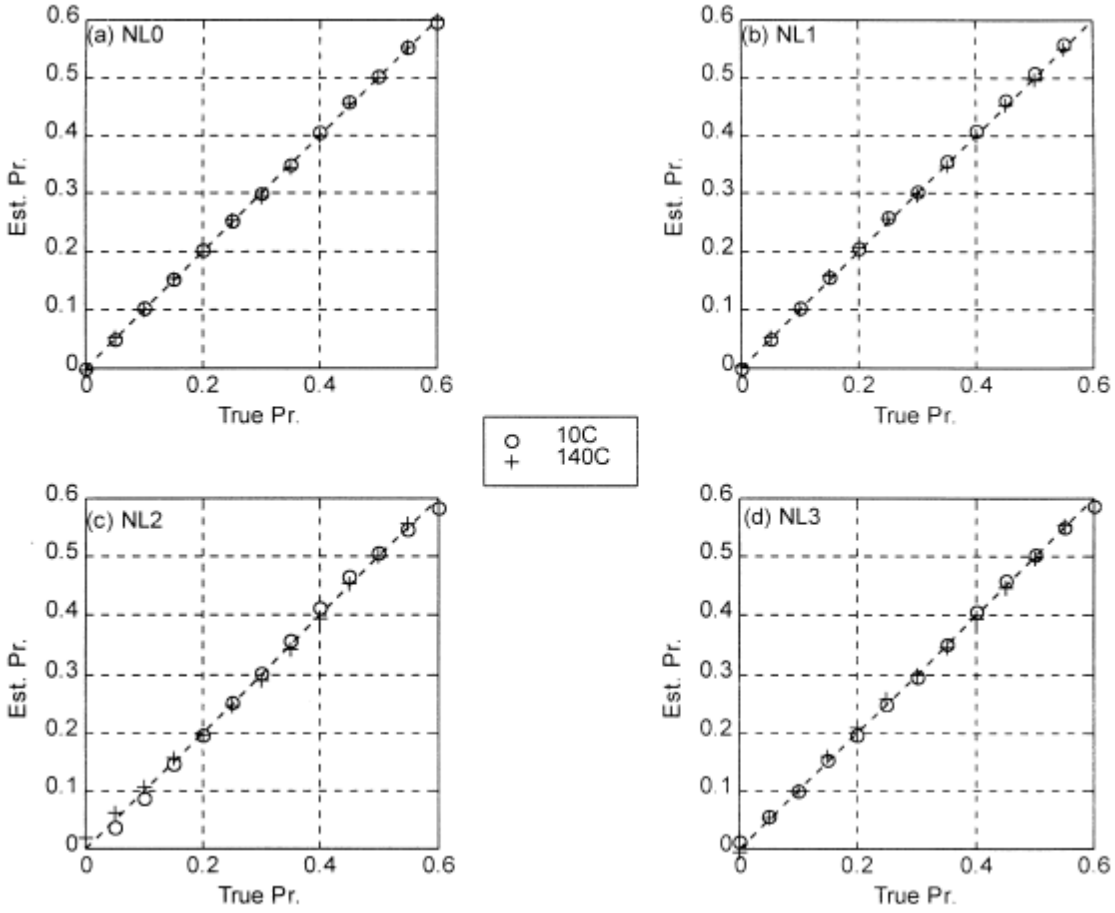

Fig. 8

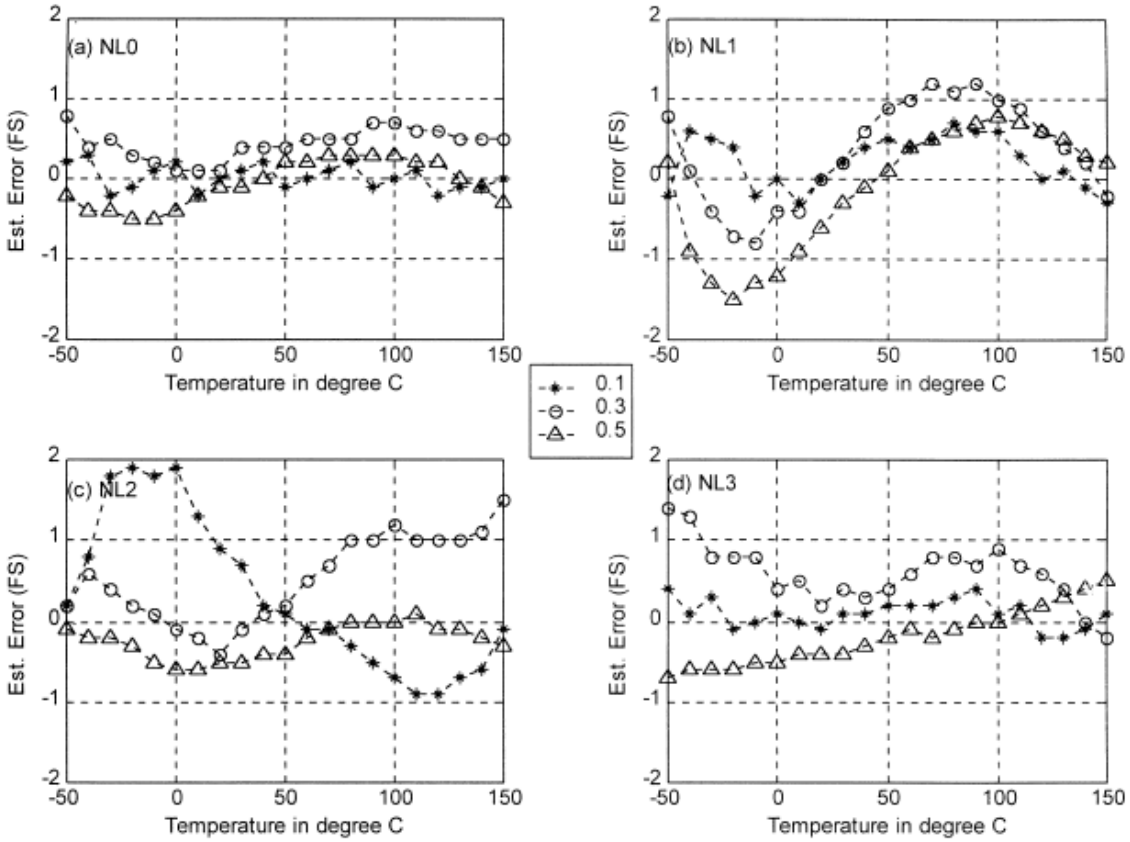
(a) NL0
(b) NL1
(c) NL2
(d) NL3
Est. Error (FS)
Temperature in degree C
0.1
0.3
0.5

Fig. 9

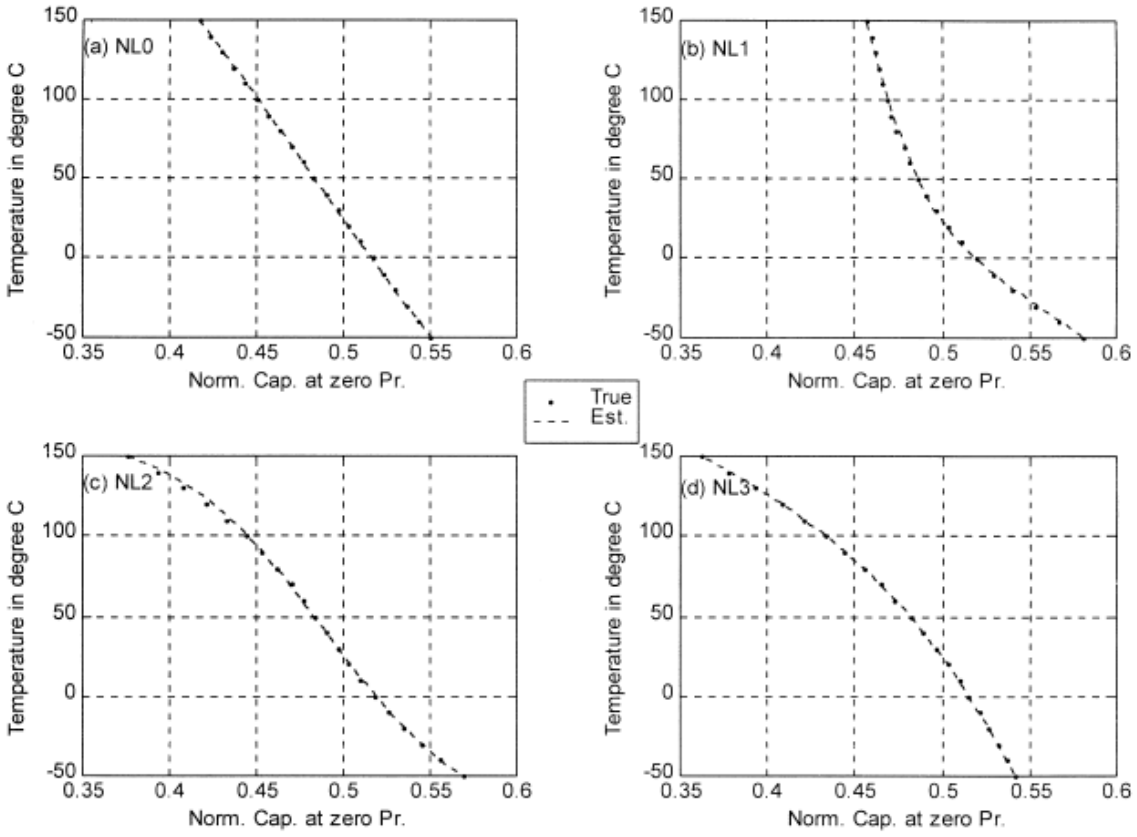
(a) NL0
(b) NL1
(c) NL2
(d) NL3
Temperature in degree C
Norm. Cap. at zero Pr.
150
100
50
0
-50
0.35
0.4
0.45
0.5
0.55
0.6
True
Est.

Fig. 10

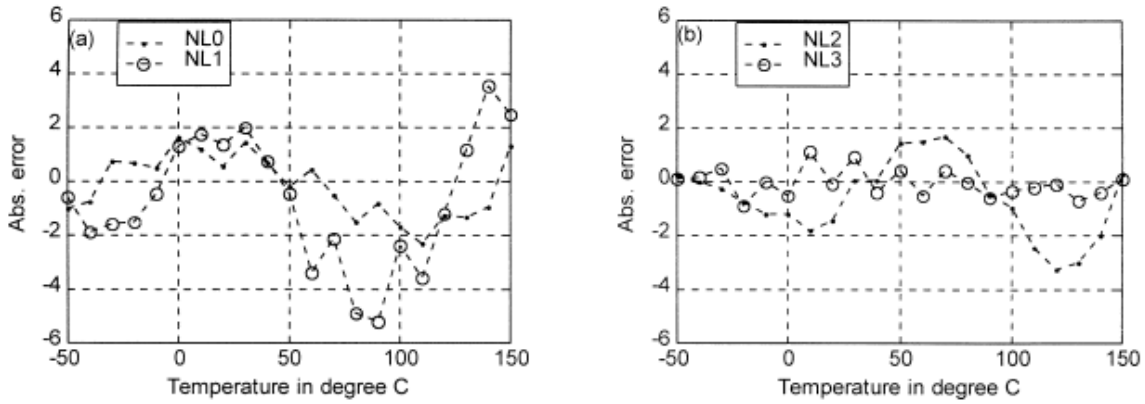
(a)
NL0
NL1
Abs. error
Temperature in degree C
(b)
NL2
NL3
Abs. error
Temperature in degree C

Fig. 11

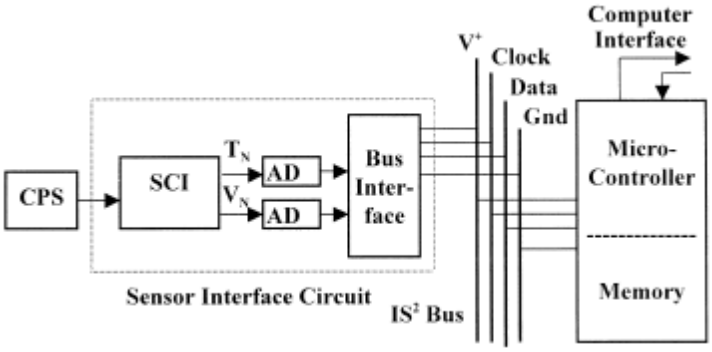
Computer
Interface
V+
Clock
Data
Gnd
CPS
SCI
TN
VN
AD
AD
Bus
Inter-
face
Micro-
Controller
Memory
Sensor Interface Circuit
IS2 Bus

Fig. 12